Electronic Supplementary Material (ESI) for Chemical Communications.

Ultrafast Labeling and High-Fidelity Imaging of Mitochondria in Cancer Cells with an Aggregation-Enhanced Emission Fluorescent Probe

Li Liu,[a] Qian Zou,[a] Jong-Kai Leung,[b] Jia-Li Wang, [a] Chuen Kam, [b] Sijie Chen,[*b] Shun Feng, [a] and Ming-Yu Wu, [*a]

a School of Life Science and Engineering, Southwest Jiaotong University, Chengdu 610031, China. E-mail: wumy1050hx@swjtu.edu.cn.

b Ming Wai Lau Centre for Reparative Medicine, Karolinska Institutet, Hong Kong, China. E-mail: sijie.chen@ki.se.

Materials and general instruments

All chemical reagents were obtained from J&K Scientific and were used without further purification. All the solvents for optical spectroscopic studies were HPLC or spectroscopic grade. TLC analyses were performed on silica gel GF 254. Column chromatography purification was carried out on silica gel (200–300 mesh). NMR spectra were recorded using a Bruker AMX-600. Chemical shifts were given in ppm relative to the internal reference TMS, $CDCl_3$ or DMSO-d_6 as the internal standard. The following abbreviations were used in ^1H NMR: s = singlet; d = doublet; t = triplet; q = quartet; m = multiplet. High resolution mass spectra were recorded on a Bruker Daltonics Bio TOF mass spectrometer. Fluorescence spectra were obtained using a Horiba Duetta spectrofluorimeter with a 10 mm quartz cuvette. UV-Vis absorption spectra were recorded on a Hitachi PharmaSpec UV-1900 UV-Visible spectrophotometer. The average particle size of the samples was recorded on a Brookhaven Zeta Plus potential analyzer at 25 $^{\circ}$C.

MTT assay for the cell cytotoxicity and phototoxicity

The cytotoxicity on HeLa cells was determined by the standard 3-(4,5-dimethylthiazol-2-yl)-2,5-diphenyl-2H-tetrazolium bromide (MTT) assay. HeLa cells were seeded at a density of 7×10^3 cells per well in 96-well black plates with 100 μL of culture medium and cultured overnight to reach 70–80% confluence. After that the medium was

replaced with 100 μL of fresh medium containing different concentrations of probes (2.5, 5, 10, 15 or 20 μM) and DMSO was used as a vehicle control. Cells were then irradiated by white LED light with a power density of around 5 mW/cm^2 for 60 min, 120 min or in the dark environment. After 24 h of incubation, 10 μL of 12 mM MTT stock solution (Sigma-Aldrich) mixed with 90 μL of PBS was added to each well for an additional 4 h of incubation. The absorbance was measured at 570 nm using a SpectraMax M2 microplate reader (Molecular Devices). Cell viability (%) was calculated as: (OD_{570} sample/OD_{570} control) × 100%.

Cell culture

HeLa, MDA-MB-231, HepG2, T47D, HEK-293T, HUVEC, and HFF cell lines were kindly provided by the State Key Laboratory of Biotherapy and Cancer Center, West China Hospital, Sichuan University. HeLa cells, MDA-MB-231 cells, HFF cells and HEK-293T cells were cultured in Dulbecco's modified Eagle's medium (DMEM) (Life Technologies) supplemented with 10% (*v*/*v*) fetal bovine serum (Life Technologies) and 1% antibiotic-antimycotic (Sigma-Aldrich). HepG2 and T47D cells were cultured in RPMI 1640 medium (Life Technologies) supplemented with 10% (*v*/*v*) fetal bovine serum and 1% antibiotics-antimycotic. HUVEC cells were cultured in vascular cell basal medium (ATCC) supplemented

with endothelial cell growth kit-BBE (ATCC). All of the cell lines were maintained in the presence of 5% CO_2 in a humidified incubator at 37 ℃.

Imaging

For confocal imaging, 4×10^3 cells were seeded in 35-mm glass-bottom dishes and cultured for 24 h. Cells were then incubated with 10 μM of LIQ probes or 5 μM TPE-Ph-In, respectively, for 30 min. After washing with PBS three times, cells were transferred to DMEM medium without phenol red (Life Technologies). Confocal imaging was performed using a Zeiss LSM 880 laser scanning confocal microscope equipped with a Plan-Apochromat 63×/1.4 NA oil objective lens, a photo-multiplier tube and a Gallium arsenide phosphide detector driven by the ZEN software (Carl Zeiss). The 488 nm laser and 560–650 nm emission filter were used for TPE-Ph-In. The 405 nm laser and 420-520 nm (**LIQ-1** and **LIQ-2**) or 500–600 nm (**LIQ**-3) emission filter were used for probes. The 488 nm laser and 500-550 nm emission filter were used for MTG. Digital images were captured with ZEN software (ZEN 2.5 lite) in grayscale and pseudocolored. Image processing was done using Adobe Photoshop (CS2).

For Co-localization analysis: Image Pro Plus 6.0 software was used for the colocalization analysis by measuring the colocalization of the merged figure in the red and green channels to create calculated correlations

between the images for the Pearson correlation coefficient and to create a color view of scatter plot

To acquire 3D images: reconstruction of Z-stack images on indicated focal planes (190 nm stepwise) were collected with Zeiss LSM 880 laser scanning confocal microscope equipped with a Plan-Apochromat 63×/1.4 NA oil objective lens, a photo-multiplier tube and a Gallium arsenide phosphide detector driven by the ZEN software (Carl Zeiss). For **AIQ-3**: λ_{ex} = 405 nm, λ_{em} = 500-600 nm. For MTG: λ_{ex} = 488 nm, λ_{em} = 500-550 nm.

Table S1 Optical properties of all probes in solvents with different polarity, in the aggregation state and solid state.

Probe	Solvent	λ_{abs} (nm)	λ_{em} （nm）	Φ_F (%)	ε (M^{-1} ·cm^{-1})	ΔSS/nm
LIQ-1	DCM	386	477	1.858	10590	91
	THF	381	474	1.209	10360	93
	EtOH	380	477	1.715	11040	97
	DMSO	384	473	0.263	10780	89
	PBS	378	476	1.350	11410	98
	AEE		475	2.23		
	Solid		484	0.12		
LIQ-2	DCM	405	476	1.796	22810	71
	THF	400	480	5.234	11960	80
	EtOH	399	476	2.001	24110	77
	DMSO	402	478	2.629	22590	76
	PBS	393	477	1.837	22940	84
	AEE		479	11.25		
	Solid		479	1.06		
LIQ-3	DCM	422	521	40.824	14344	99
	THF	413	550	9.098	11240	137
	EtOH	415	545	14.222	13890	131
	DMSO	418	563	7.032	13334	145
	PBS	405	556	2.374	13180	151
	AEE		560	18.9		
	Solid		518	13.44		

Absorption and emission maximum were measured in dichloromethane. AEE：aggregation state Fluorescence quantum yields were determined using quinine sulfate in 0.1 M sulphuric acid as a standard (Φ_F = 0.55).

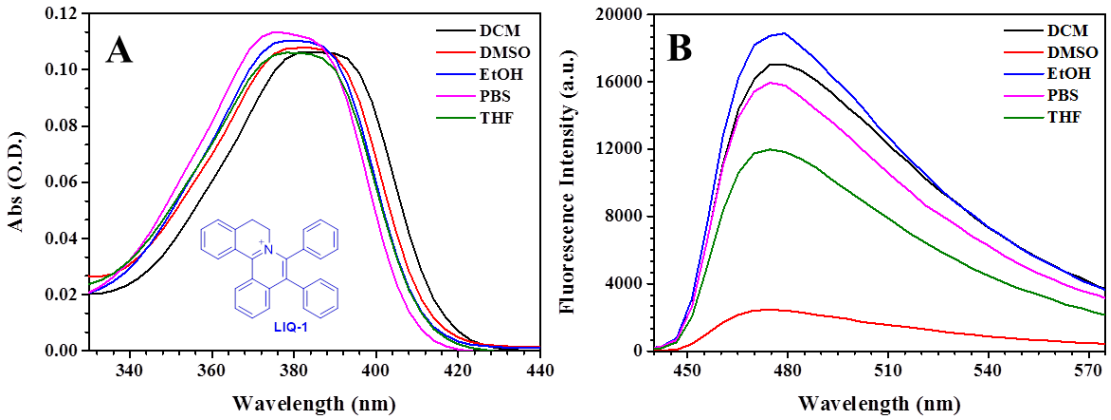

Fig. S1 (A) UV-vis spectra and (B) fluorescence spectra of **LIQ-1** (10 μM) in DCM, THF, EtOH, DMSO and PBS solution. Excitation wavelength = 386 nm (DCM), 384 nm (DMSO), 380 nm (EtOH), 378 nm (PBS), 381 nm (THF).

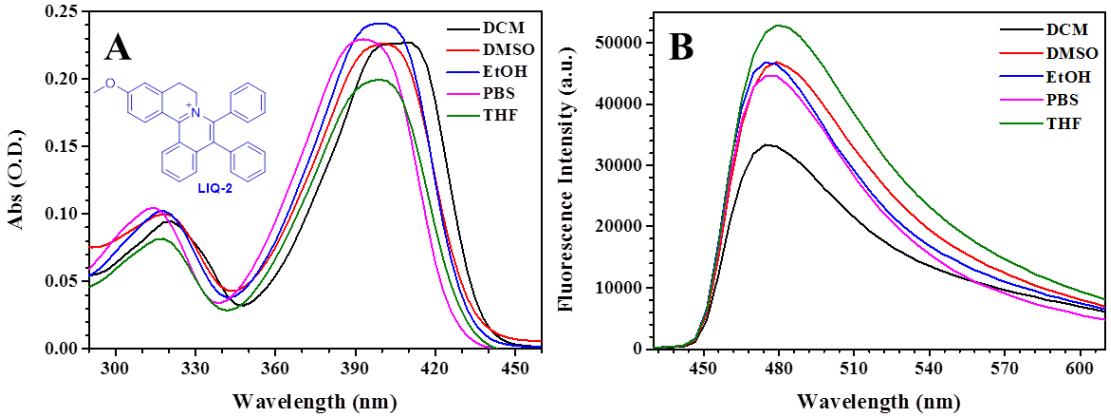

Fig. S2 (A) UV-vis spectra and (B) fluorescence spectra of **LIQ-2** (10 μM) in DCM, THF, EtOH, DMSO and PBS solution. Excitation wavelength = 405 nm (DCM), 402 nm (DMSO), 399 nm (EtOH), 393 nm (PBS), 400 nm (THF).

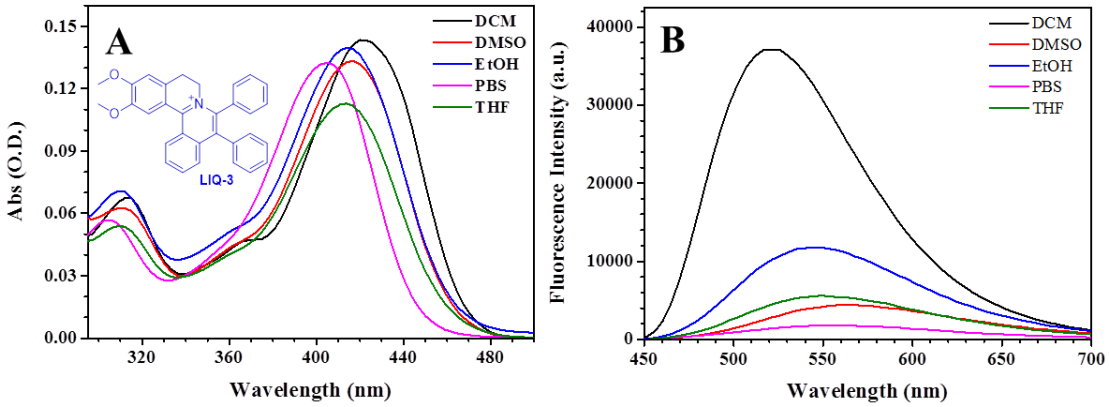

Fig. S3 (A) UV-vis spectra and (B) fluorescence spectra of **LIQ-3** (10 μM) in DCM, THF, EtOH, DMSO and PBS solution. Excitation wavelength = 422 nm (DCM), 418 nm (DMSO), 415 nm (EtOH), 405 nm (PBS), 413 nm (THF).

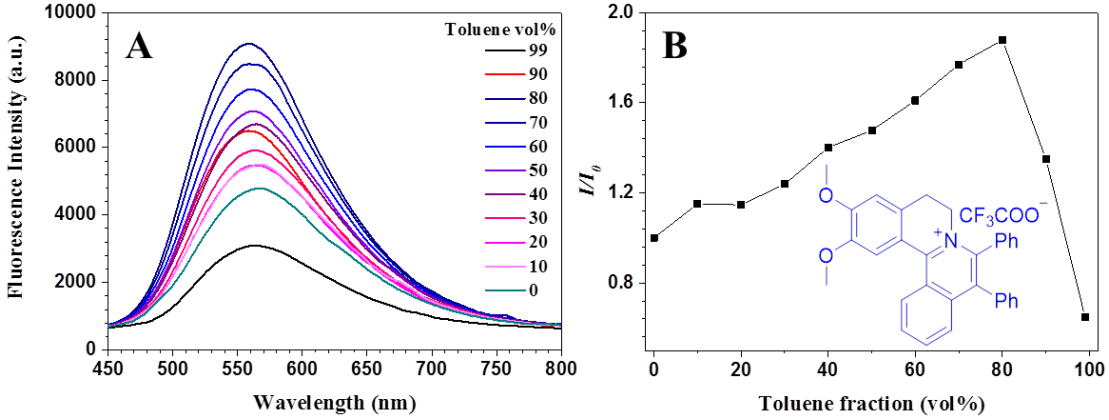

Fig. S4 (A) Fluorescence spectra of **LIQ-3** (10 μM) in DMSO/toluene mixtures. (B) Plots of fluorescence intensity ratio (I/I_0) versus toluene fractions of **LIQ-3** in mixtures of DMSO/toluene with different toluene fractions. I_0, emission intensity in DMSO; λ_{ex} = 418 nm.

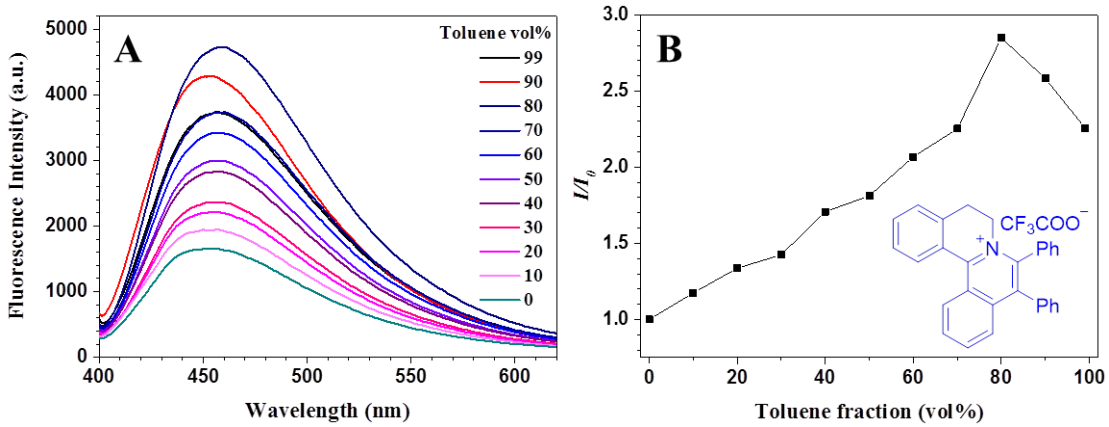

Fig. S5 (A) Fluorescence spectra of **LIQ-1** (10 μM) in DMSO/toluene mixtures. (B) Plots of fluorescence intensity ratio (I/I_0) versus toluene fractions of **LIQ-1** in mixtures of DMSO/toluene with different toluene fractions. I_0, emission intensity in DMSO; λ_{ex} = 384 nm.

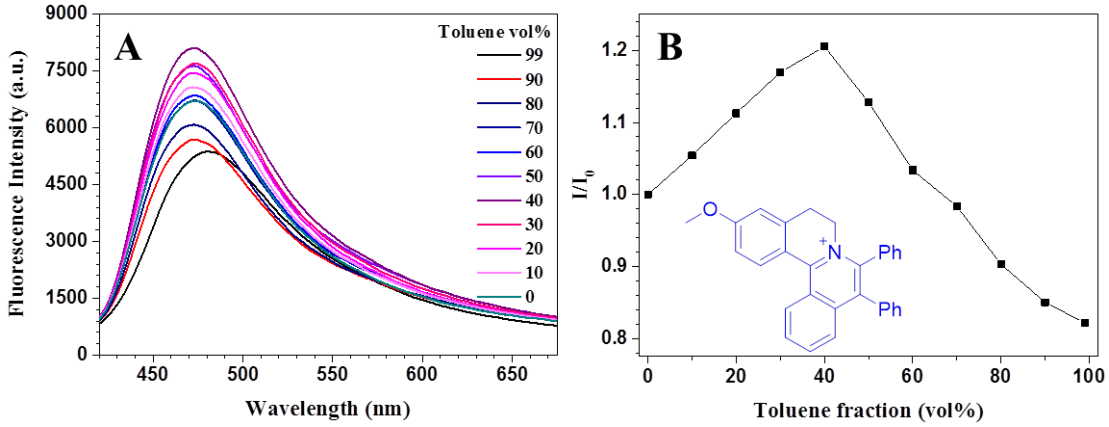

Fig. S6 (A) Fluorescence spectra of **LIQ-2** (10 μM) in DMSO/toluene mixtures. (B) Plots of fluorescence intensity ratio (I/I_0) versus toluene fractions of **LIQ-2** in mixtures of DMSO/toluene with different toluene fractions. I_0, emission intensity in DMSO; λ_{ex} = 402 nm.

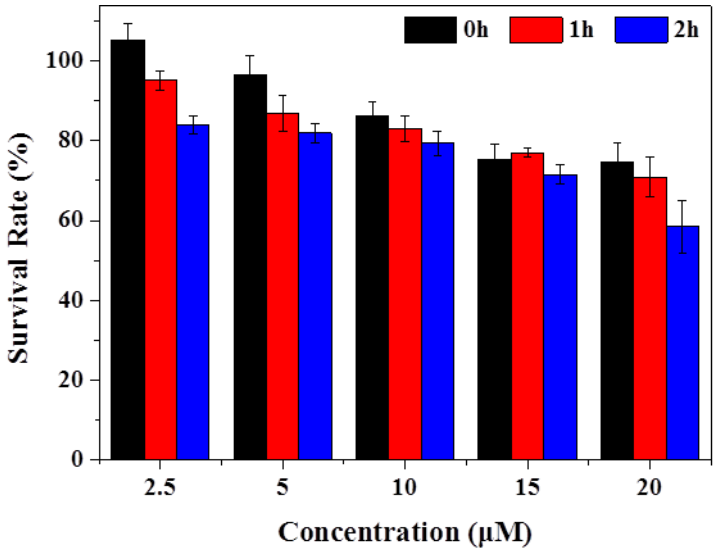

Fig. S7 HeLa cells were incubated with different concentrations of **LIQ-1** (2.5, 5, 10, 15, 20 μM) in the absence or presence of white LED light irradiation (5 mW/cm^2) for 1 h or 2 h. Cell survival rates was determined by the MTT assay.

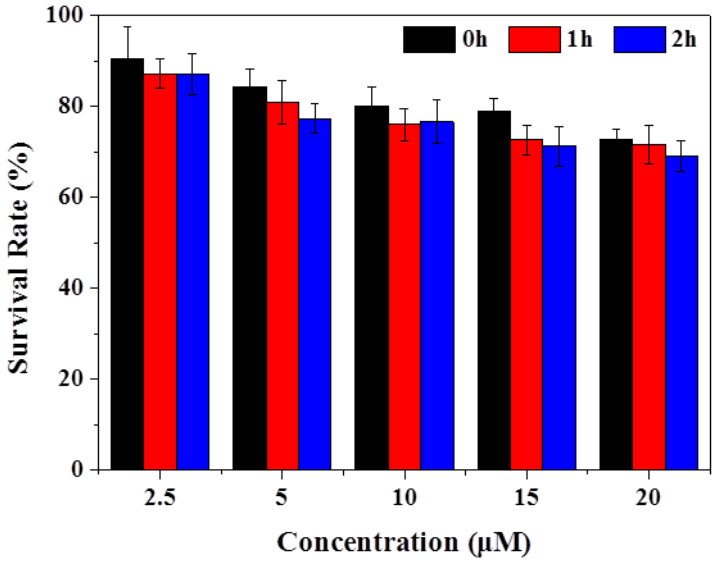

Fig. S8 HeLa cells were incubated with different concentrations of **LIQ-2** (2.5, 5, 10, 15, 20 μM) in the absence or presence of white LED light irradiation (5 mW/cm^2) for 1 h or 2 h. Cell survival rates was determined by the MTT assay.

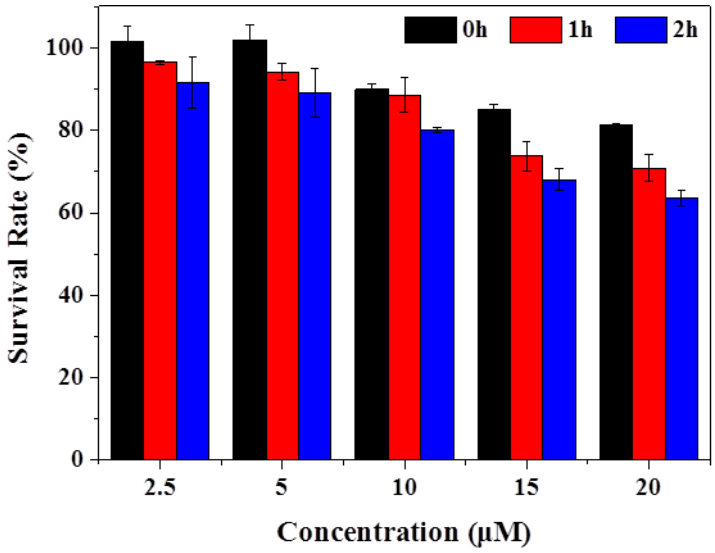

Fig. S9 HeLa cells were incubated with different concentrations of **LIQ-3** (2.5, 5, 10, 15, 20 μM) in the absence or presence of white LED light irradiation (5 mW/cm^2) for 1 h or 2 h. Cell survival rates was determined by the MTT assay.

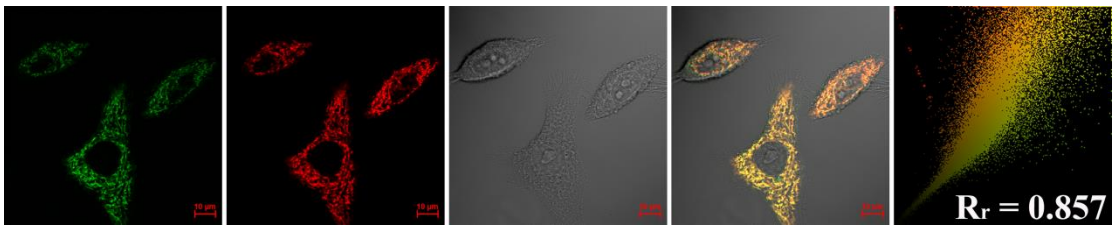

Fig. S10 Co-localization of **LIQ-1** (10 μM) with TPE-Ph-In (5 μM) in HeLa cells. **LIQ-1** (green) and TPE-Ph-In (red) colocalized with each other on mitochondrial structures. The scatter plot displays the correlation between red and green pixel intensities of cells shown in both channels. Degree of colocalization was determined by Pearson's correlation coefficient (R_r). **LIQ-1** (λ_{ex} = 405 nm, λ_{em} = 420-520 nm); TPE-Ph-In (λ_{ex} = 488 nm, λ_{em} = 620-720 nm).

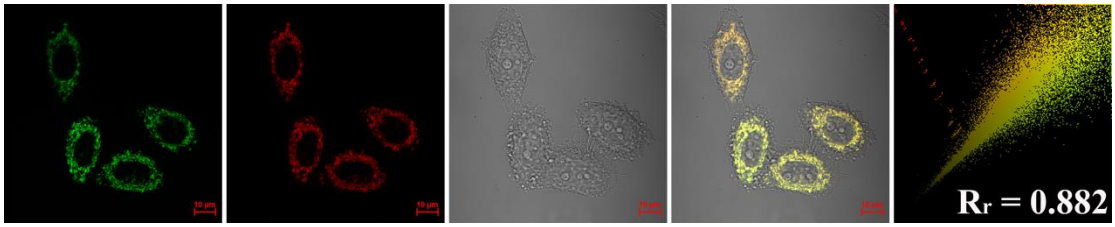

Fig. S11 Co-localization of **LIQ-2** (10 μM) with TPE-Ph-In (5 μM) in HeLa cells. **LIQ-2** (green) and TPE-Ph-In (red) colocalized with each other on mitochondrial structures. The scatter plot displays the correlation between red and green pixel intensities of cells shown in both channels. Degree of colocalization was determined by Pearson's correlation coefficient (R_r). **LIQ-2** (λ_{ex} = 405 nm, λ_{em} = 420-520 nm); TPE-Ph-In (λ_{ex} = 488 nm, λ_{em} = 620-720 nm).

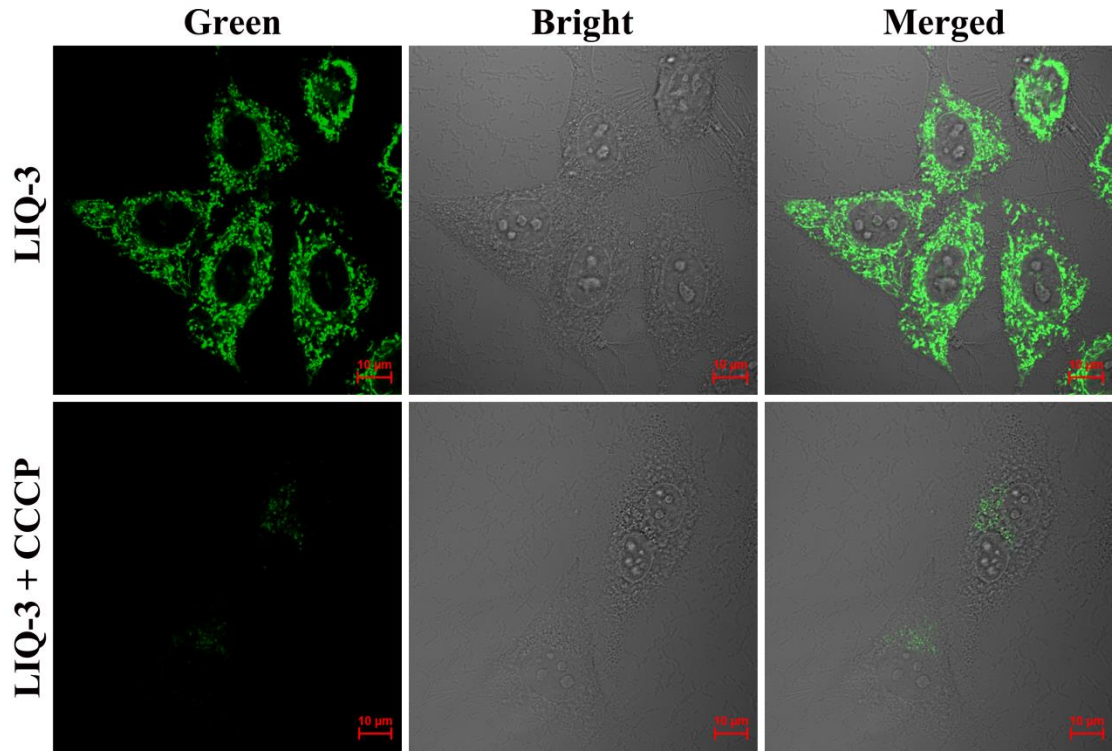

Fig. S12 Fluorescent images of HeLa cells after stained with **LIQ-3** (10 μM, 30 min) and treated without CCCP or treated with 50 μM CCCP for 15 min. λ_{ex} = 405 nm, λ_{em} = 500-600 nm.

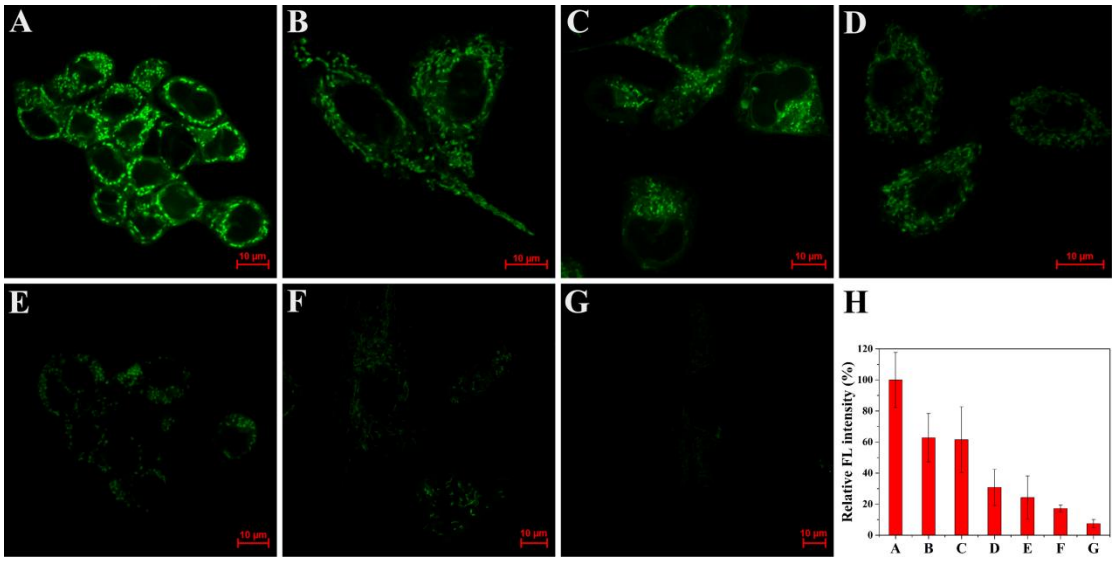

Fig. 13 Differentiation of cancer cells from normal cells by **LIQ-3**. (A–G) Fluorescence images of different cancer cells and normal cells stained with **LIQ-3** for 30 min. (H) Quantification of relative fluorescence intensity of **LIQ-3** in different cell lines relative to that in T47D cells. (Data were from the corresponding images in A-G. A: T47D, B: HeLa, C: MDA-MB-231, D: HepG2, E: HEK-293T, F: HFF, G: HUVEC).

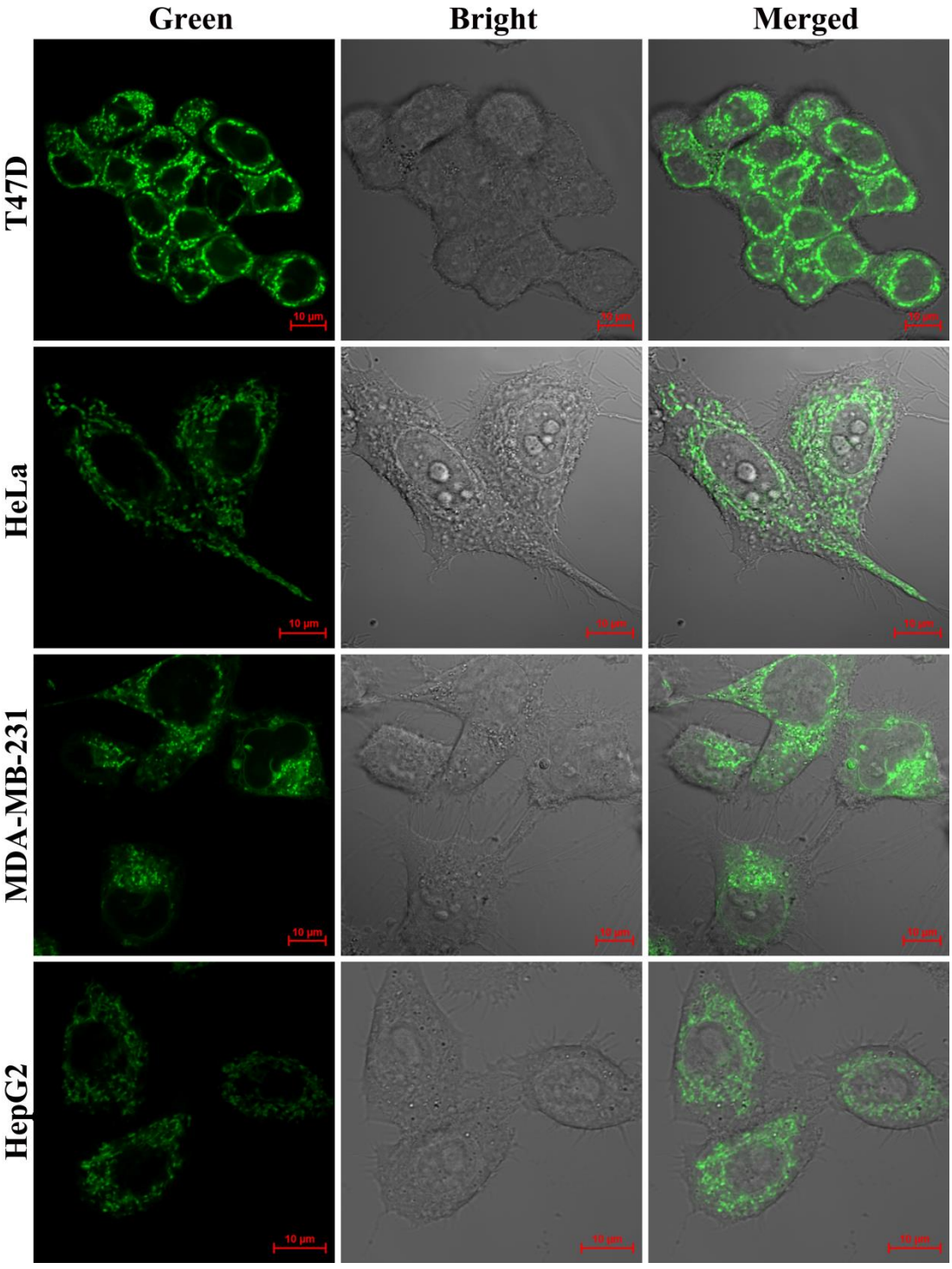

Fig. S14 Fluorescence images of different cancer cells (T47D, HeLa, MDA-MB-231 and HepG2 cells) with **LIQ-3** (10 μM) for 30 min. (λ_{ex} = 405 nm, λ_{em} = 500-600 nm).

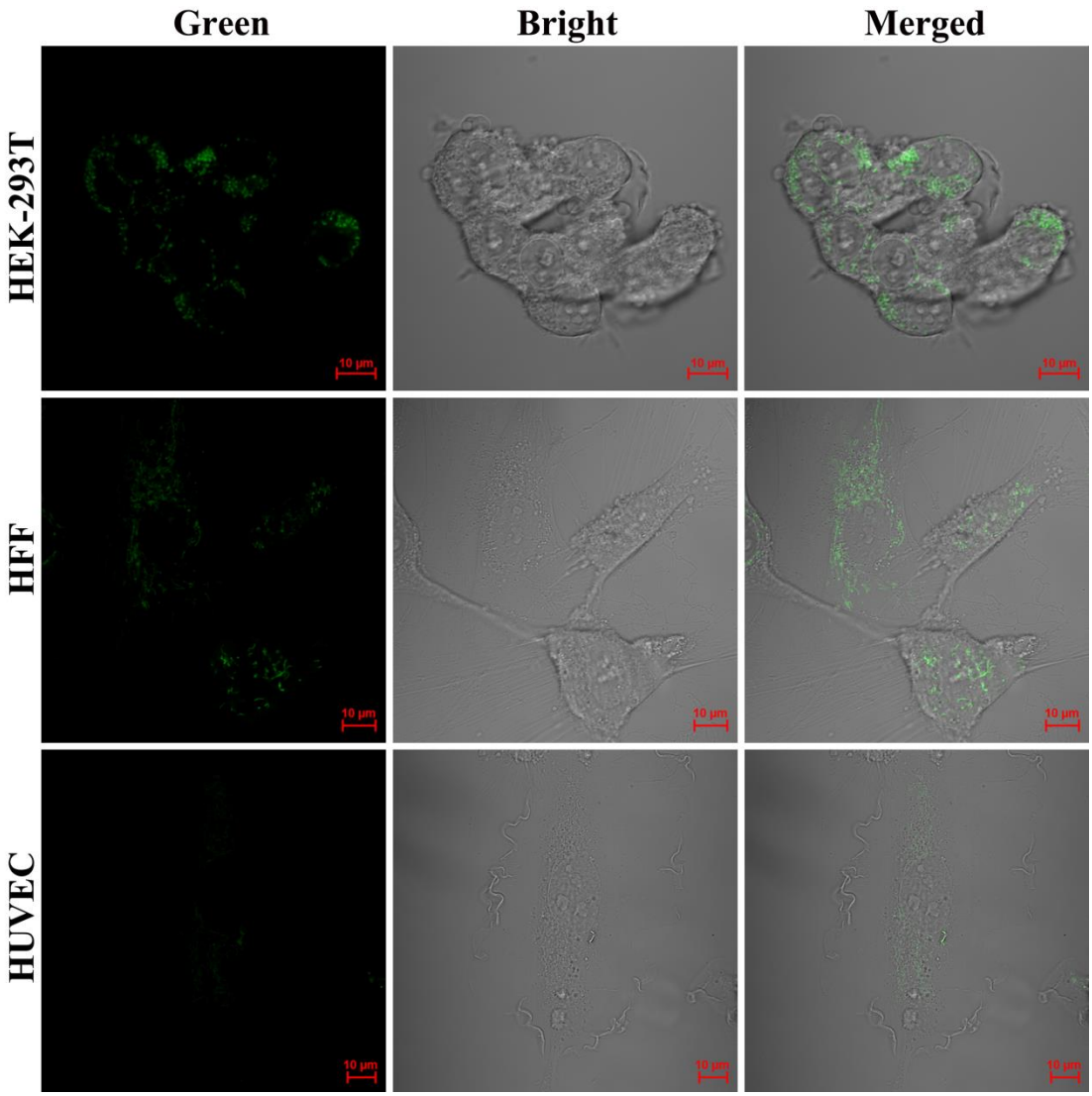

Fig. S15 Fluorescence images of different normal cells (HEK-293T, HFF and HUVEC cells) with **LIQ-3** (10 μM) for 30 min. (λ_{ex} = 405 nm, λ_{em} = 500-600 nm).

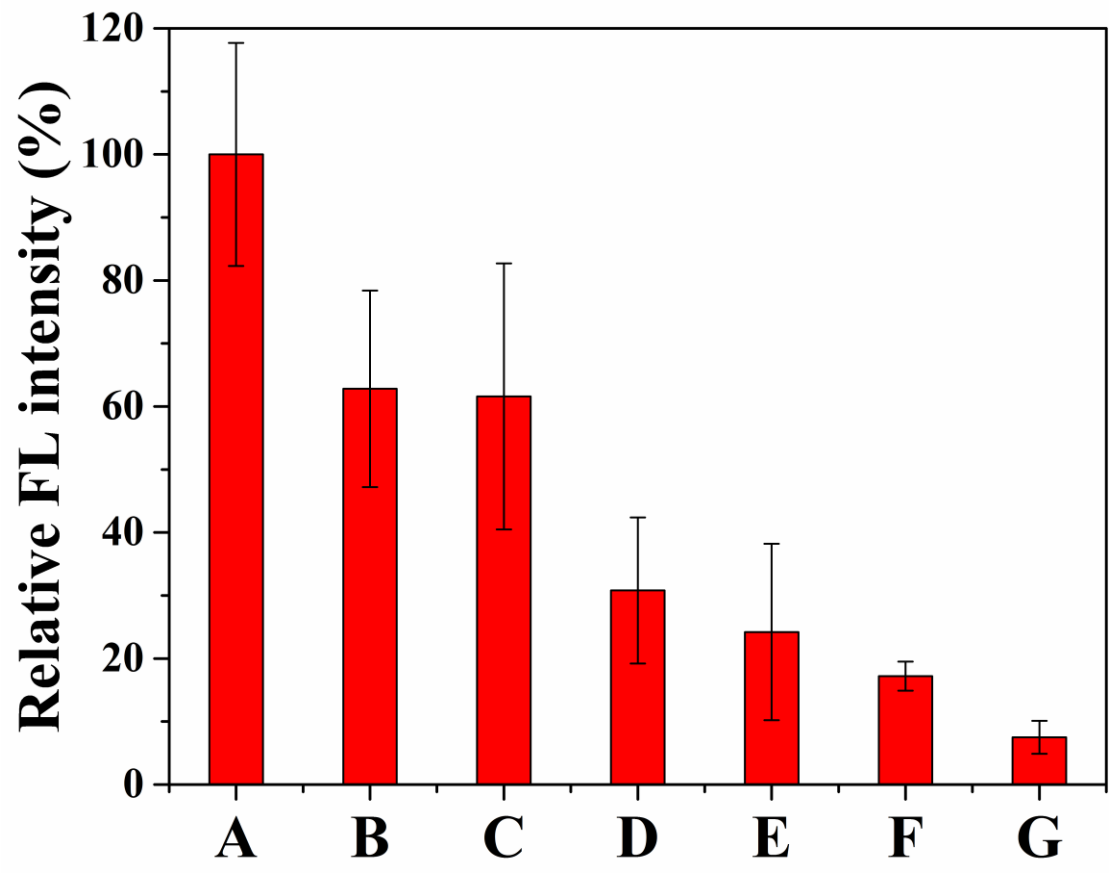

Fig. S16 Quantification of relative fluorescence intensity of **LIQ-3** in different cell lines relative to that in T47D cells. (A: T47D, B: HeLa, C: MDA-MB-231, D: HepG2, E: HEK-293T, F: HFF, G: HUVEC).

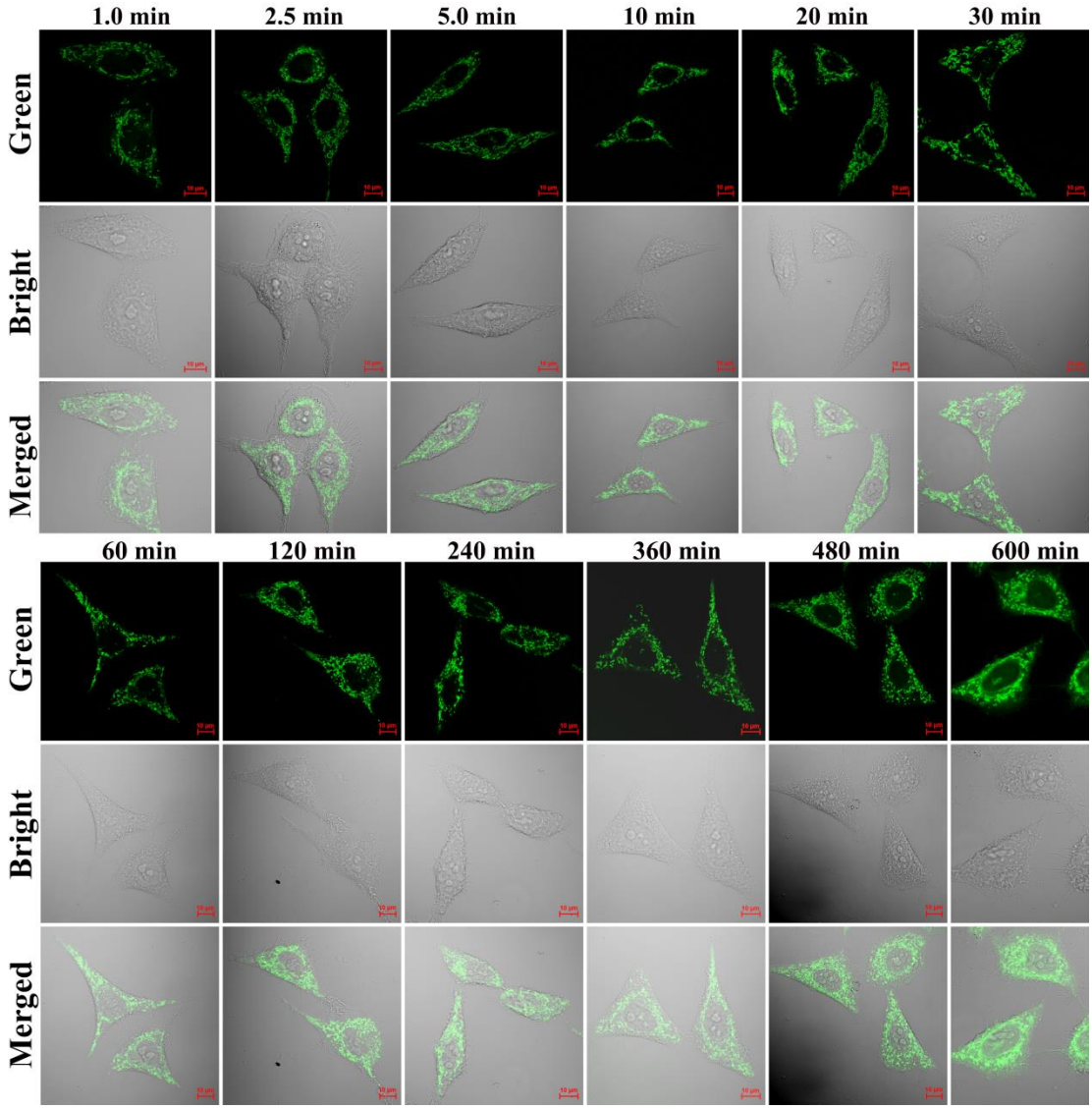

Fig. S17 Dynamic staining images of HeLa cells incubated with **LIQ-3** (10 μM) from 1 min to 600 min. Ultrafast labeling of mitochondria could be achieved by **LIQ-3** in one minute. (λ_{ex} = 405 nm, λ_{em} = 500-600 nm).

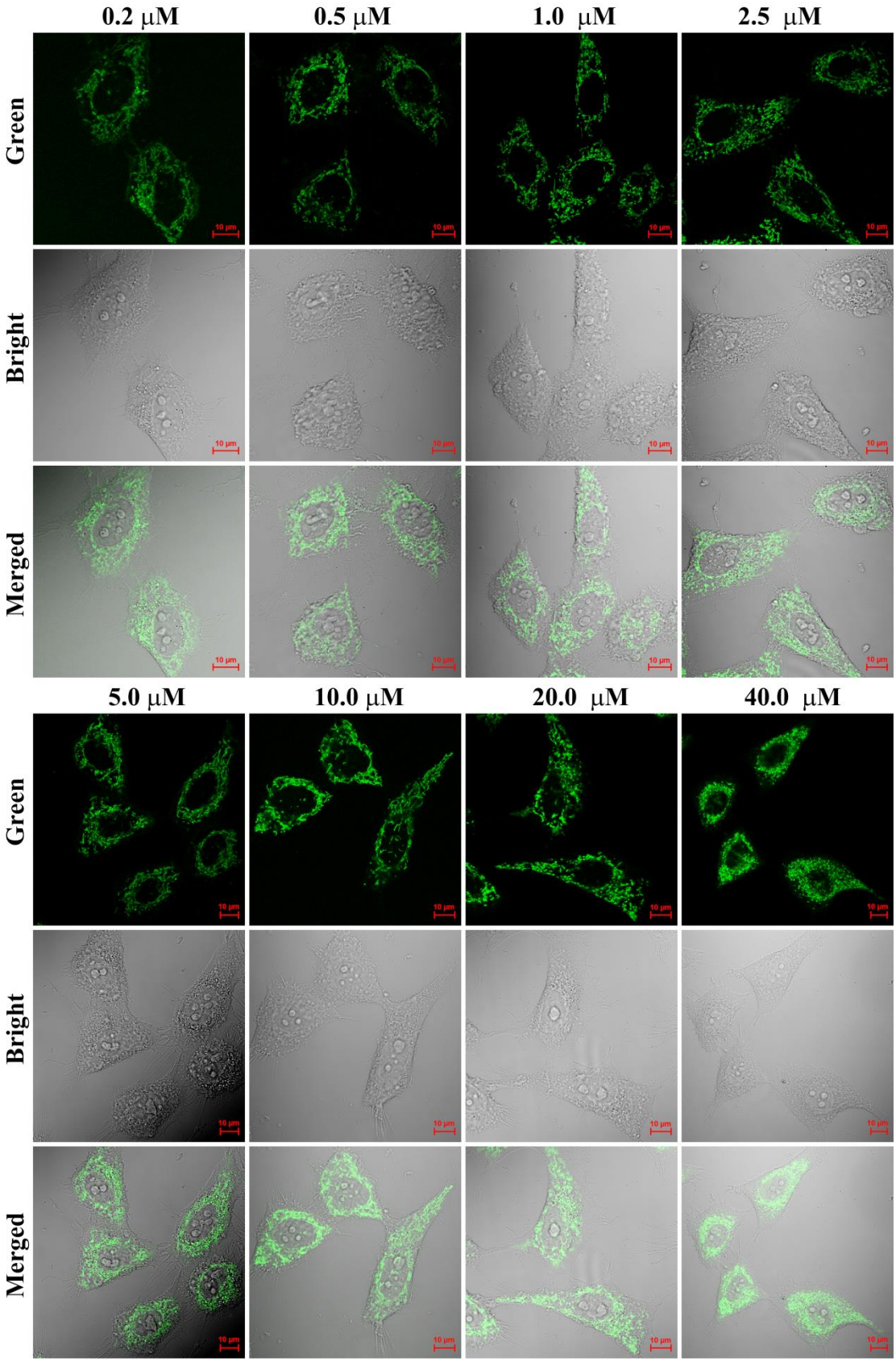

Fig. S18 High sensitivity and high-fidelity images of mitochondrial in HeLa cells labeled with different concentration of **LIQ-3** from 200 nM to 40 μM for 30 min.

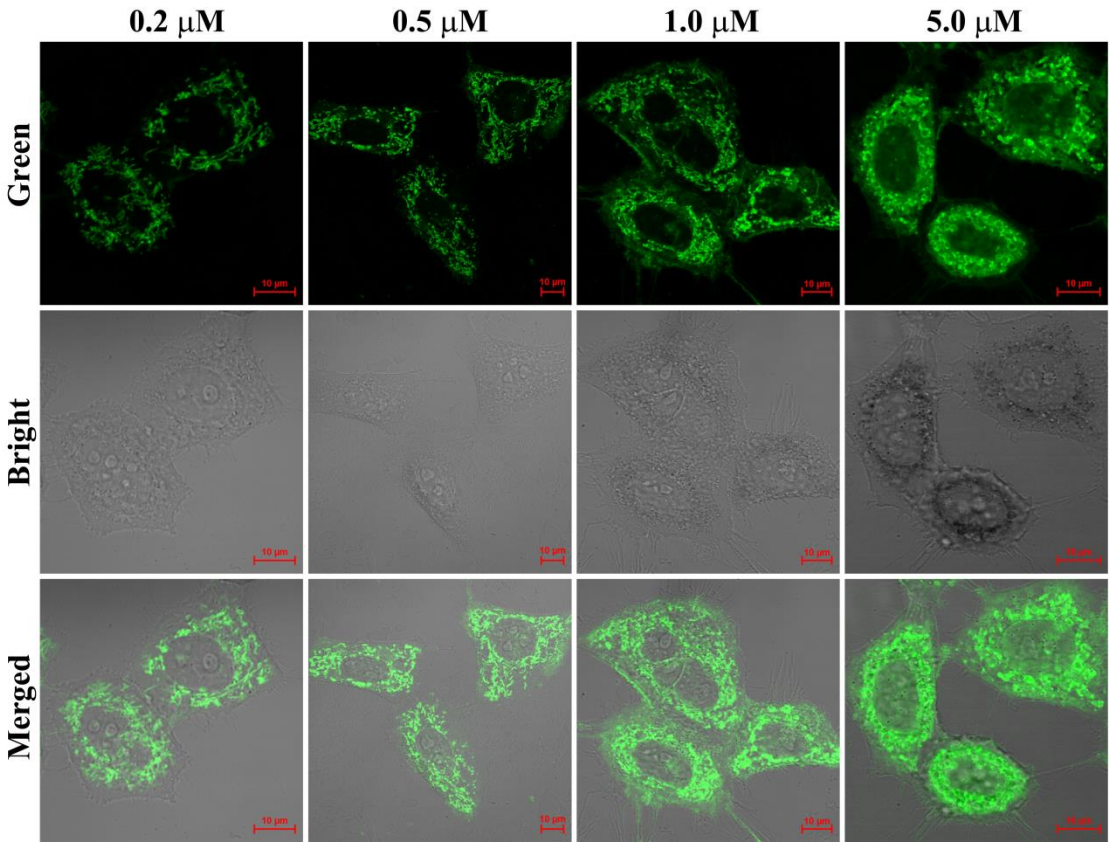

Fig. S19 Fluorescence images of mitochondria in HeLa cells labeled with different concentrations of MTG from 200 nM to 5.0 μM for 30 min. (λ_{ex} = 488 nm, λ_{em} = 500-550 nm).

Synthesis and Characterization of fluorescence probes

To 10 mL of ethyl alcohol, 0.5 mmol dihydroisoquinoline derivative[1], 0.5 mmol 1,2-diphenylethyne, 0.005 mmol $[(Cp^*RhCl_2)_2$, 0.75 mmol silver trifluoroacetate, and 0.5 mmol copper acetate were added. After heated to reflux with magnetic stirring for 30 min under N_2, the reaction mixture was filtered through diatomite and washed with ethanol. The solvent was evaporated under reduced pressure, and the crude product was purified by column chromatography on silica gel (DCM to DCM/MeOH = 20/1, *v*/*v*) to afford the product.

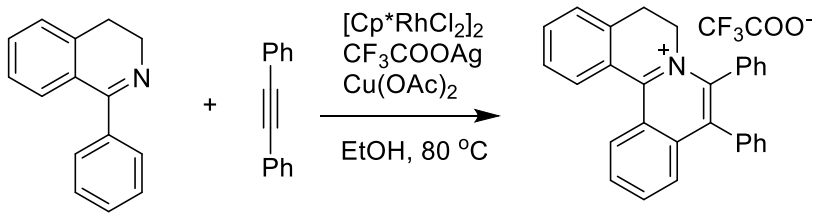

LIQ-1: light brown solid, 88 % yield. ^{1}H NMR (600 MHz, $CDCl_3$), δ. 8.68 (d, 1H, *J* = 8.4Hz), 8.03 (d, 1H, *J* = 7.8 Hz), 7.98 (d, 1H, *J* = 7.2 Hz), 7.93 (t, 1H, *J* = 7.2 Hz), 7.76 (d, 1H, *J* = 8.4 Hz), 7.71 (t, 1H, *J* = 7.2 Hz), 7.62 (t, 1H, *J* = 7.2 Hz), 7.55 (d, 1H, *J* = 7.2 Hz), 7.45-7.44 (m, 2H), 7.37 (m, 3H), 7.33-7.28 (m, 3H), 7.23-7.22 (m, 2H), 4.46 (t, 2H, *J* = 6.0Hz), 3.30 (t, 2H, *J* = 6.0 Hz). ^{13}C NMR (100 MHz, DMSO-d_6), δ. 157.7 (q, *J* = 30 Hz) (158.0, 157.8, 157.6, 157.4), 153.5, 144.3, 139.1, 138.0, 137.4, 136.2, 135.9, 134.0, 133.7, 133.4, 132.0, 130.9, 130.8, 130.3, 130.2, 129.9, 128.6, 128.4, 128.2, 128.0, 127.5, 126.6, 126.2, 125.3, 124.6, 117.3 (q, *J* = 300 Hz) (120.3, 118.3, 116.3, 114.3), 52.5, 26.5. ^{19}F NMR (DMSO-d_6), δ. -73.51. HRMS (ESI): m/z $[M - CF_3COO^-]^+$ calcd for $C_{29}H_{22}N$: 384.1747; found 384.1751.

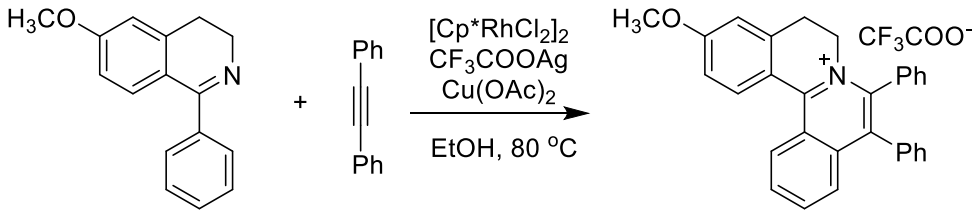

LIQ-2: Yellow solid, 96 % yield. ^{1}H NMR (600MHz, $CDCl_3$), δ. 8.63 (d, 1H, *J* = 8.4 Hz), 7.96-7.89 (m, 3H), 7.70 (d, 1H, *J* = 8.4 Hz), 7.37-7.30 (m, 8H), 7.18 (d, 2H, *J* = 5.4 Hz), 7.13 (d, 1H, *J* = 8.4 Hz), 7.10 (s, 1H),

4.40 (s, 2H), 3.98 (s, 3H), 3.27 (s, 2H). ^{13}C NMR (150MHz, $CDCl_3$), δ. 164.5, 154.3, 144.0, 141.3, 138.7, 135.9, 135.6, 135.5, 133.8, 131.5, 131.0, 130.4, 130.4, 130.3, 130.1, 129.1, 128.5, 128.4, 127.0, 125.1, 119.2, 114.2, 113.2, 56.1, 52.2, 27.8. ^{19}F NMR ($CDCl_3$), δ.-75.38. HRMS (ESI): m/z $[M - CF_3COO^-]^+$ calcd for $C_{30}H_{24}NO$: 414.1852; found 414.1842.

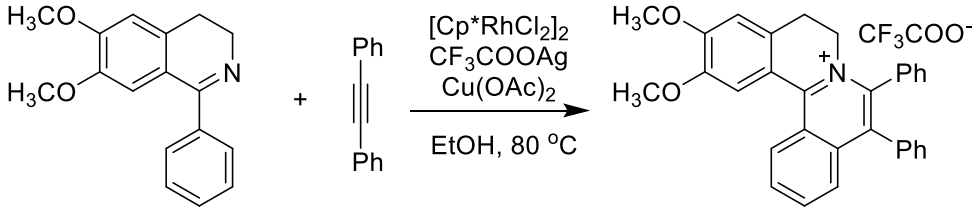

LIQ-3: yellow solid，93 % yield. ^{1}H NMR (600MHz, $CDCl_3$), δ. 8.69 (d, 1H, *J* = 8.4Hz), 7.96 (d, 1H, *J* = 7.2 Hz), 7.91 (1H, t, *J* = 7.2 Hz), 7.72 (d, 1H, *J* = 7.8 Hz), 7.49 (s, 1H), 7.42-7.20 (m, 10H), 7.12 (s, 1H), 4.42 (s, 2H), 4.06 (s, 3H), 3.97 (s, 3H), 3.26 (s, 2H). ^{13}C NMR (150MHz, $CDCl_3$), δ. 160.6 (q, *J* = 30 Hz) (160.9, 160.7, 160.5, 160.3), 154.5, 154.0, 148.4, 144.2, 138.9, 136.0, 135.5, 133.8, 133.6, 131.5, 130.6, 130.4, 130.3, 130.2, 130.1, 129.1, 128.5, 128.4, 127.2, 125.0, 120.0, 116.1, 110.9, 117.0 (q, *J* = 300 Hz) (120.0, 118.0, 116.1, 114.1), 56.7, 56.6, 52.3, 27.1. ^{19}F NMR ($CDCl_3$): δ. -74.94. HRMS (ESI): m/z $[M-CF_3COO^-]^+$ calcd for $C_{31}H_{26}NO_2$: 444.1958; found 444.1947.

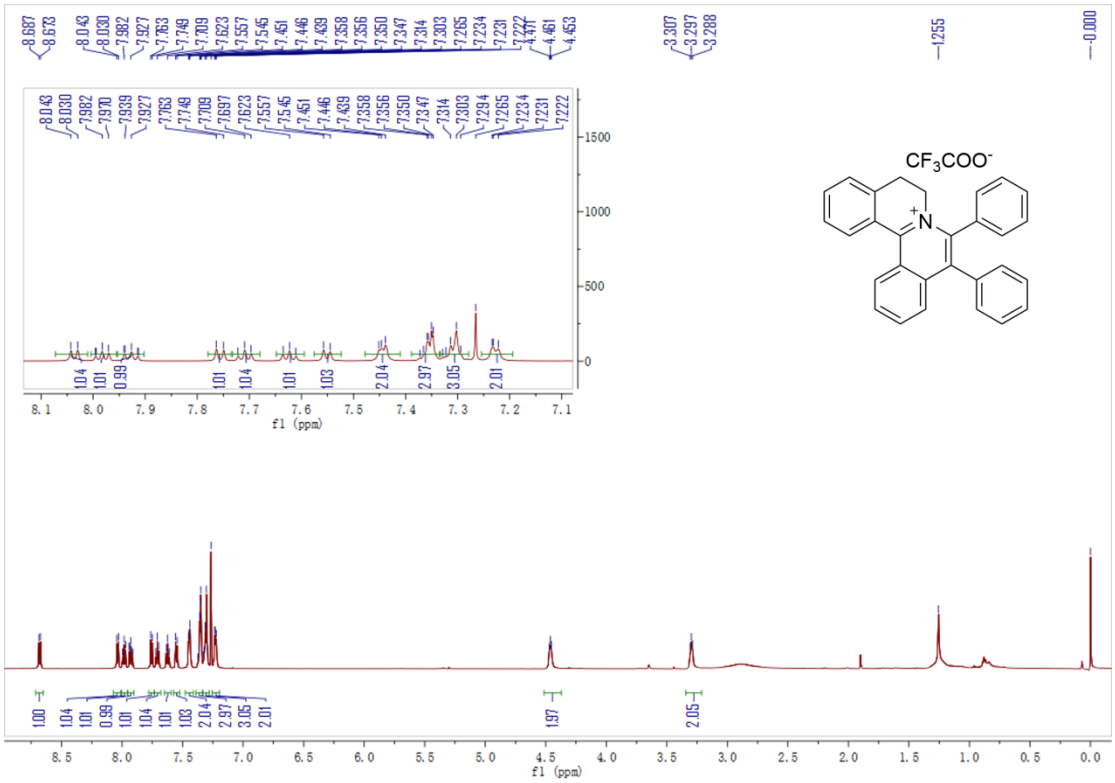

^{1}H NMR spectrum of **LIQ-1** in $CDCl_3$.

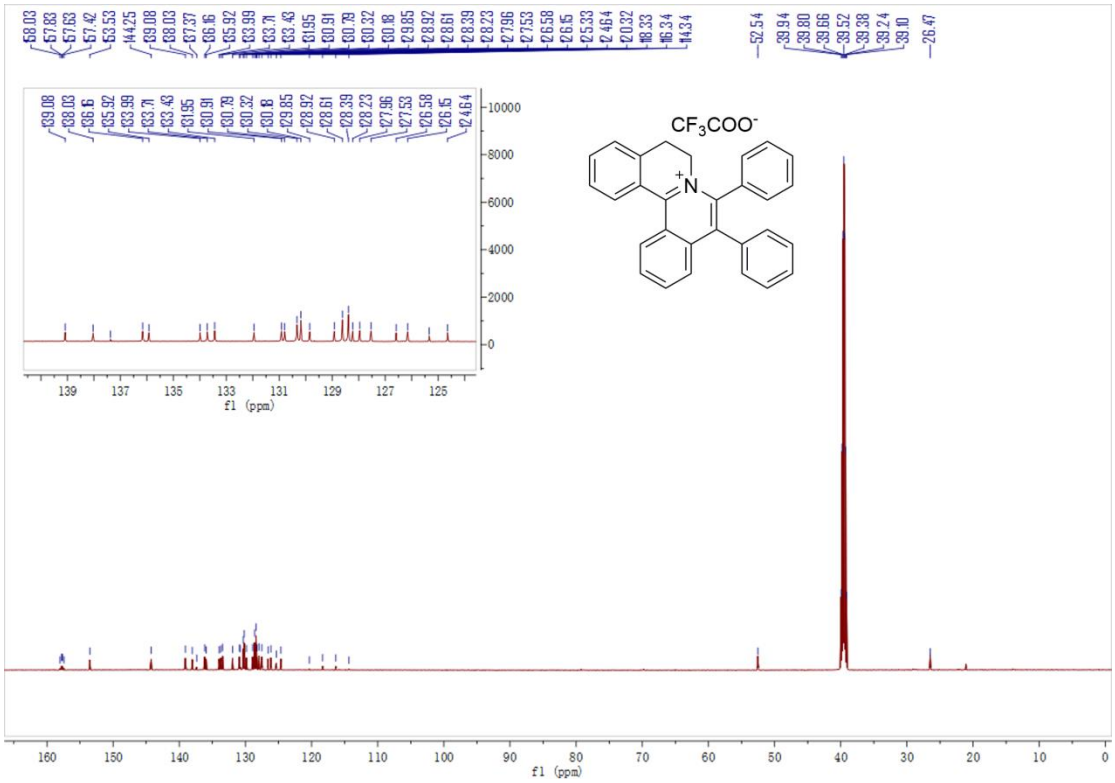

^{13}C NMR spectrum of **LIQ-1** in DMSO-d_6.

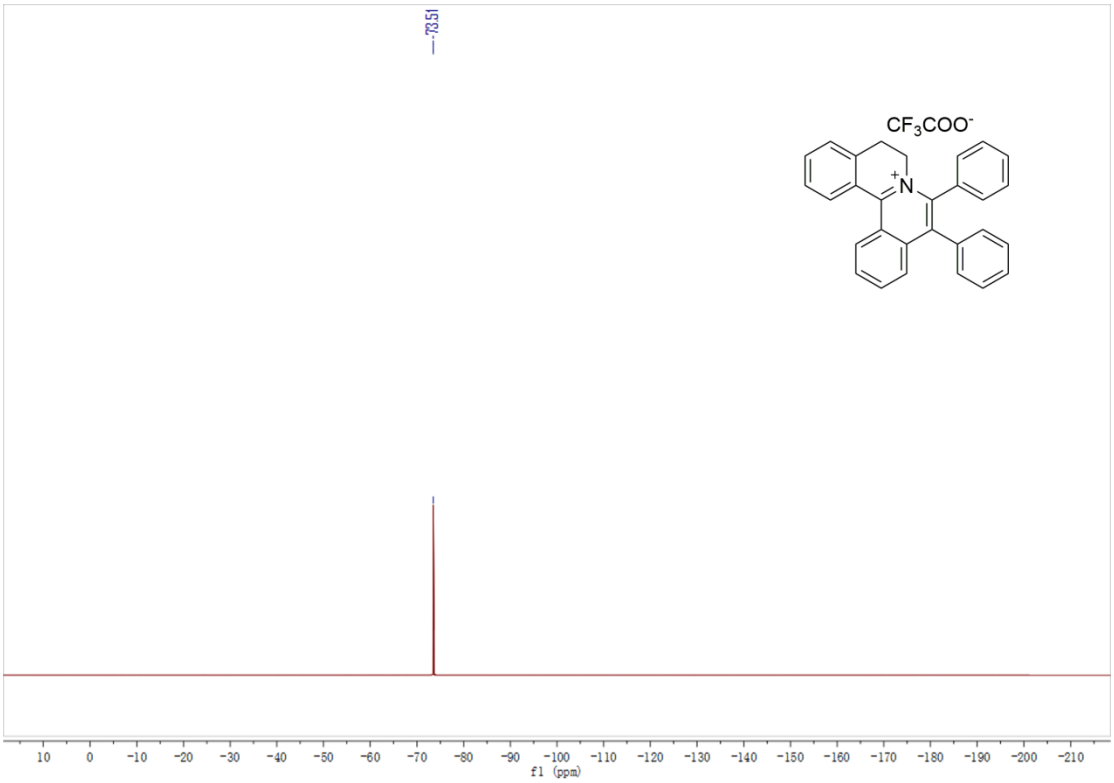

^{19}F NMR spectrum of **LIQ-1** in DMSO-d_6.

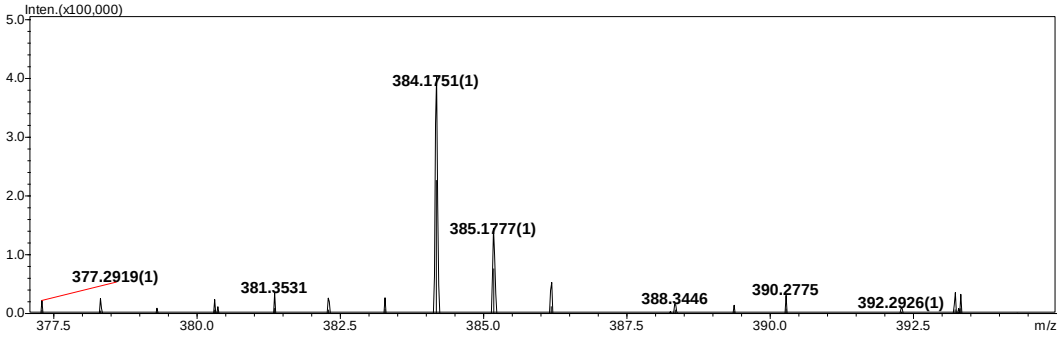

HRMS spectrum of **LIQ-1**.

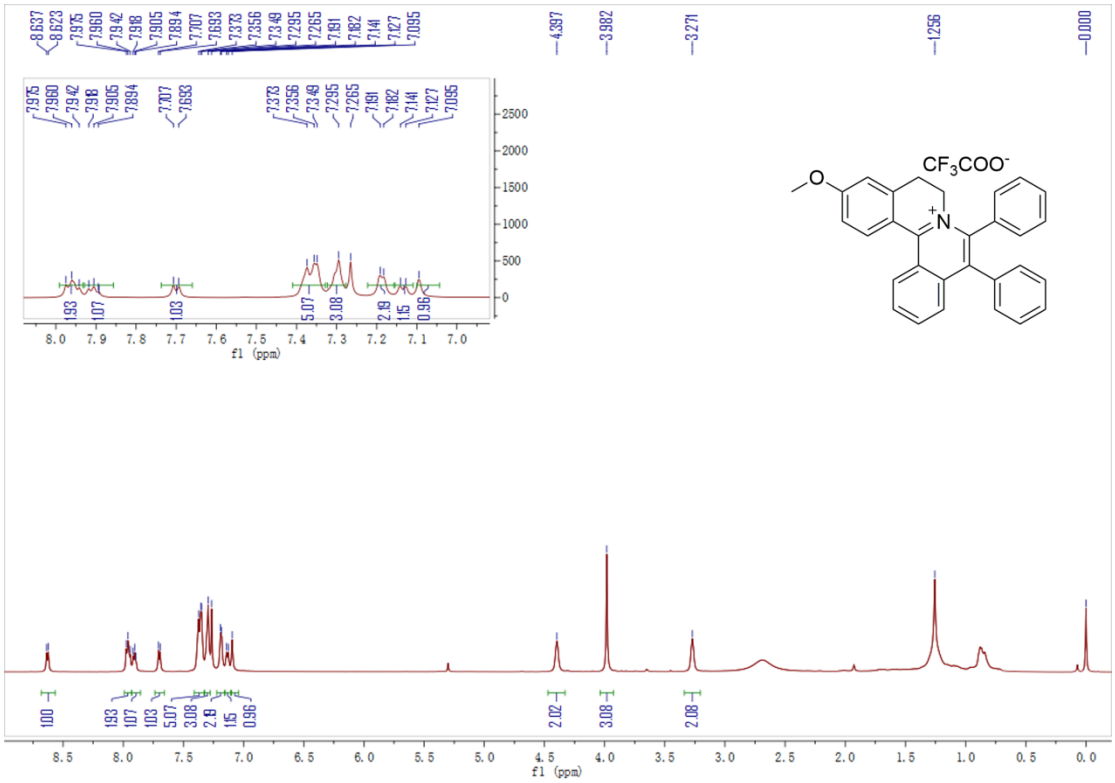

^{1}H NMR spectrum of **LIQ-2** in $CDCl_3$.

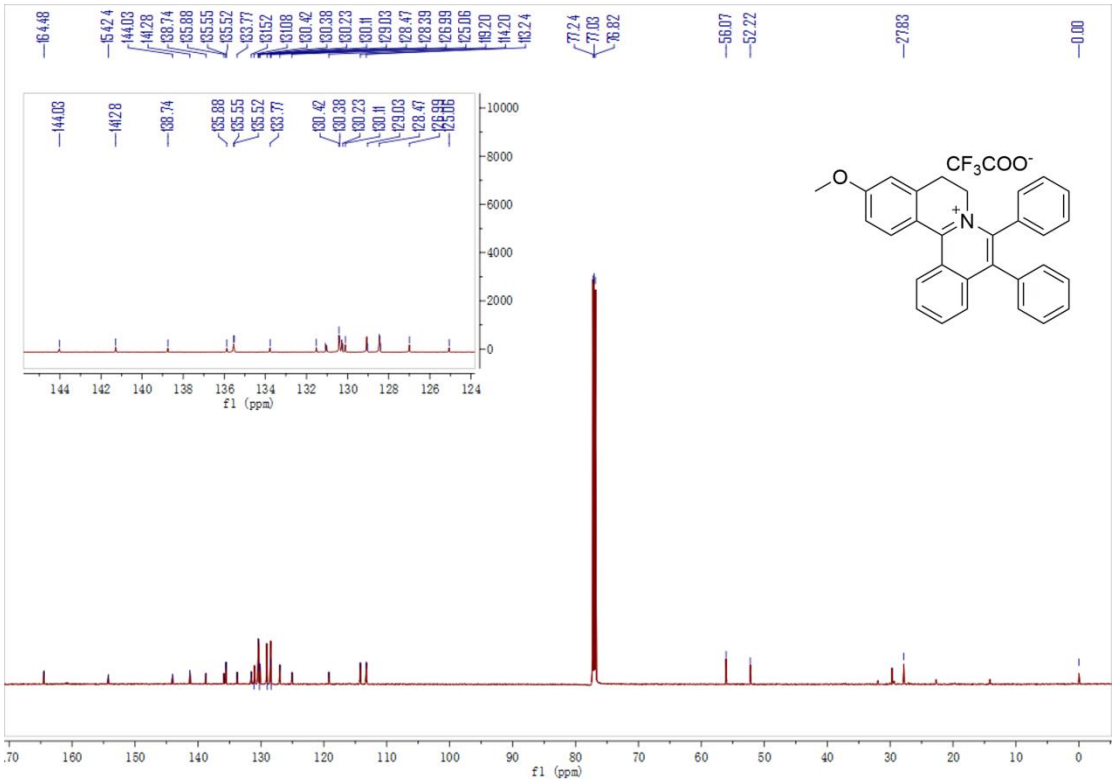

^{13}C NMR spectrum of **LIQ-2** in $CDCl_3$.

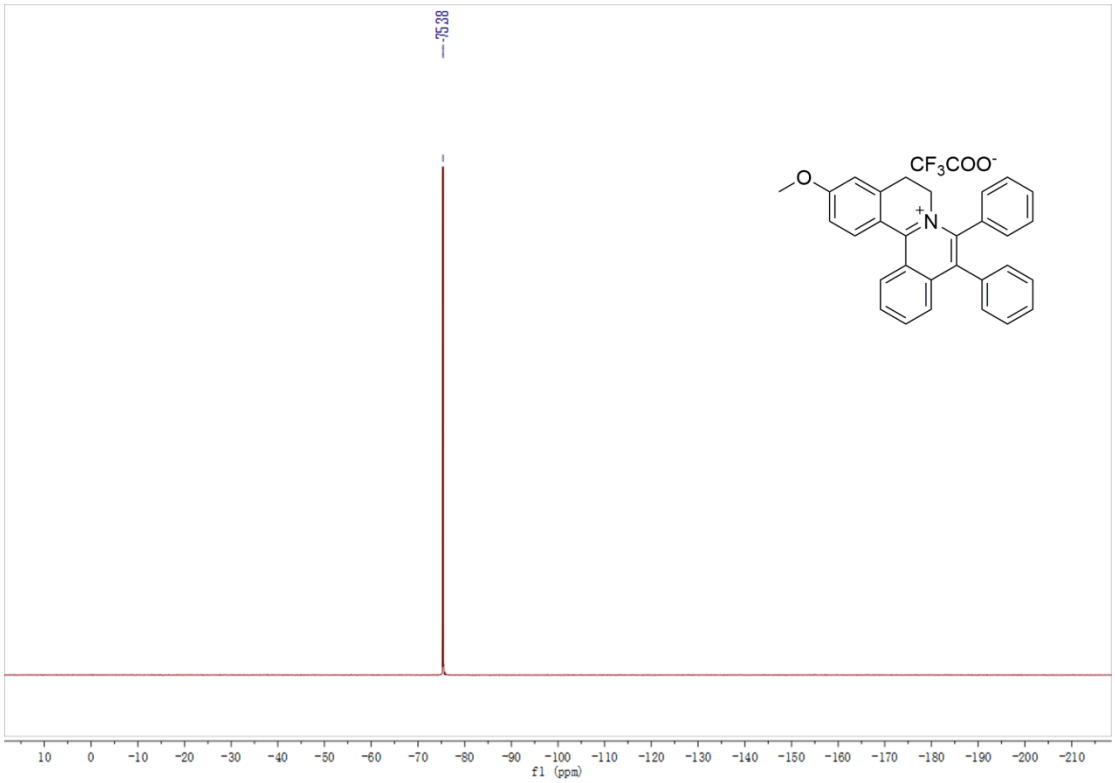

^{19}F NMR spectrum of **LIQ-2** in $CDCl_3$.

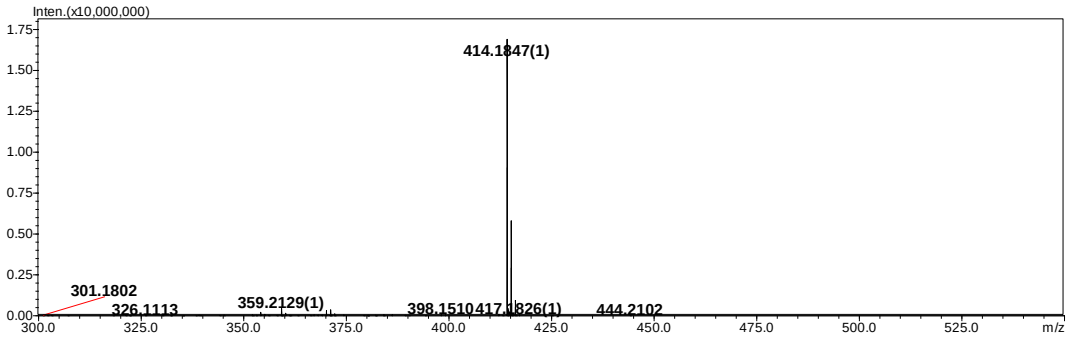

HRMS spectrum of **LIQ-2**.

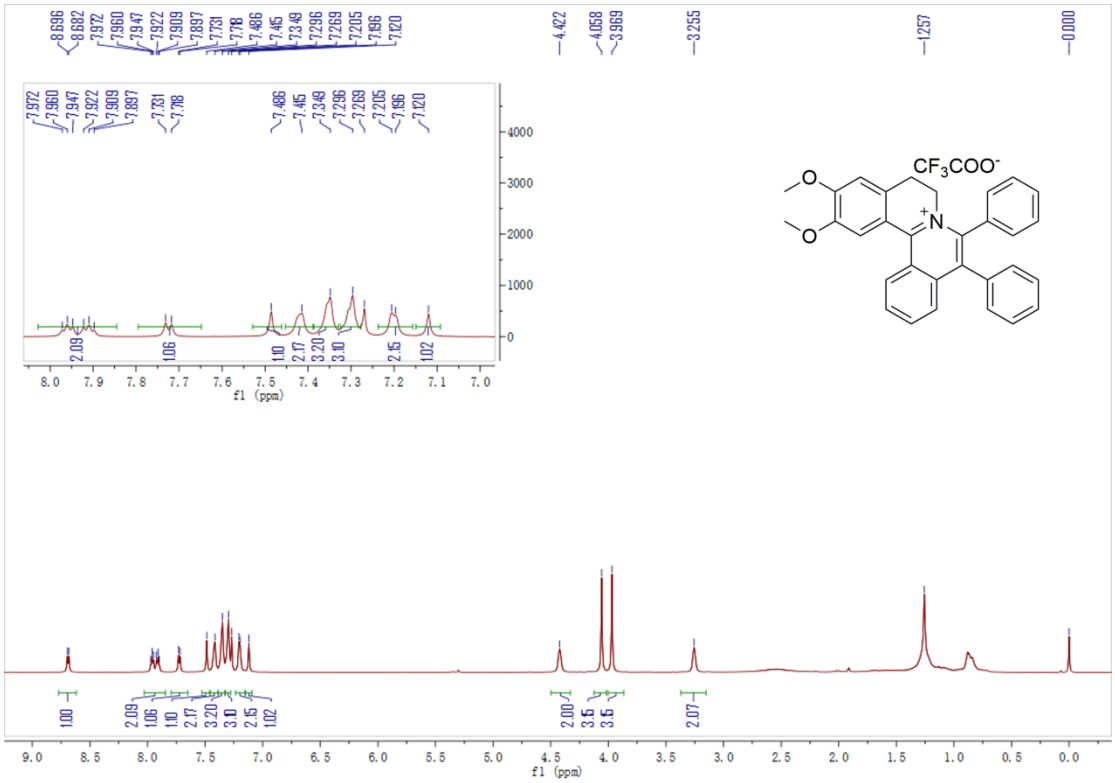

^{1}H NMR spectrum of **LIQ-3** in $CDCl_3$.

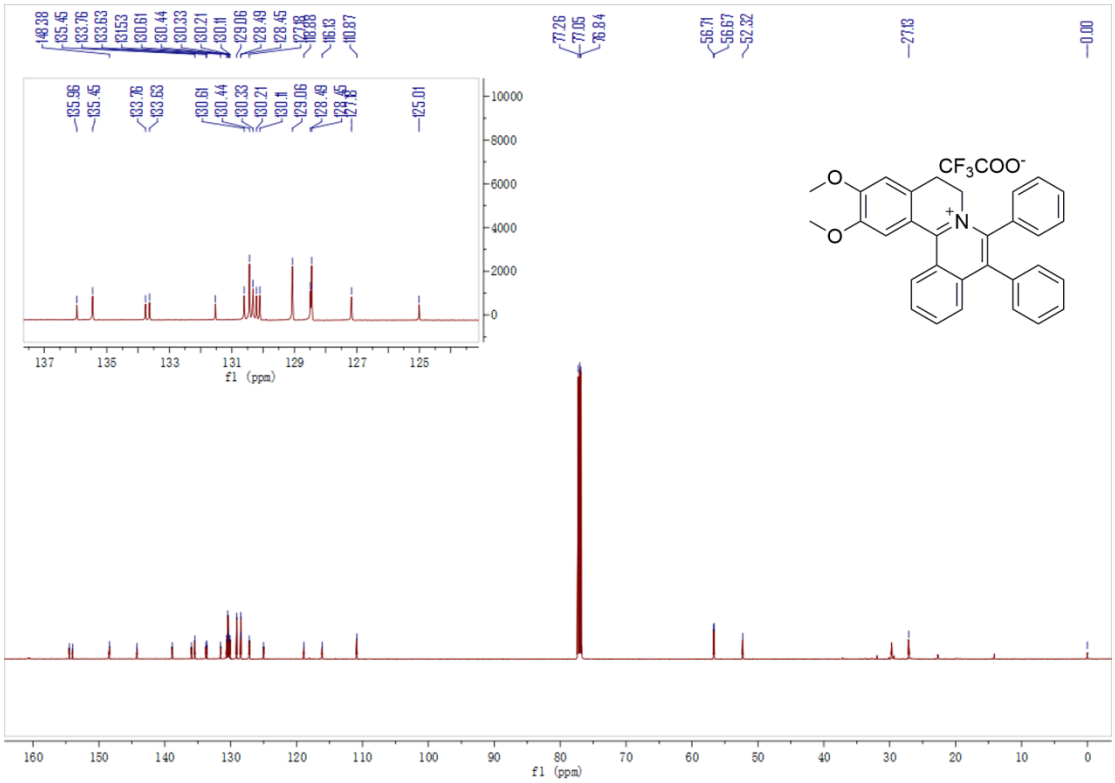

^{13}C NMR spectrum of **LIQ-3** in $CDCl_3$.

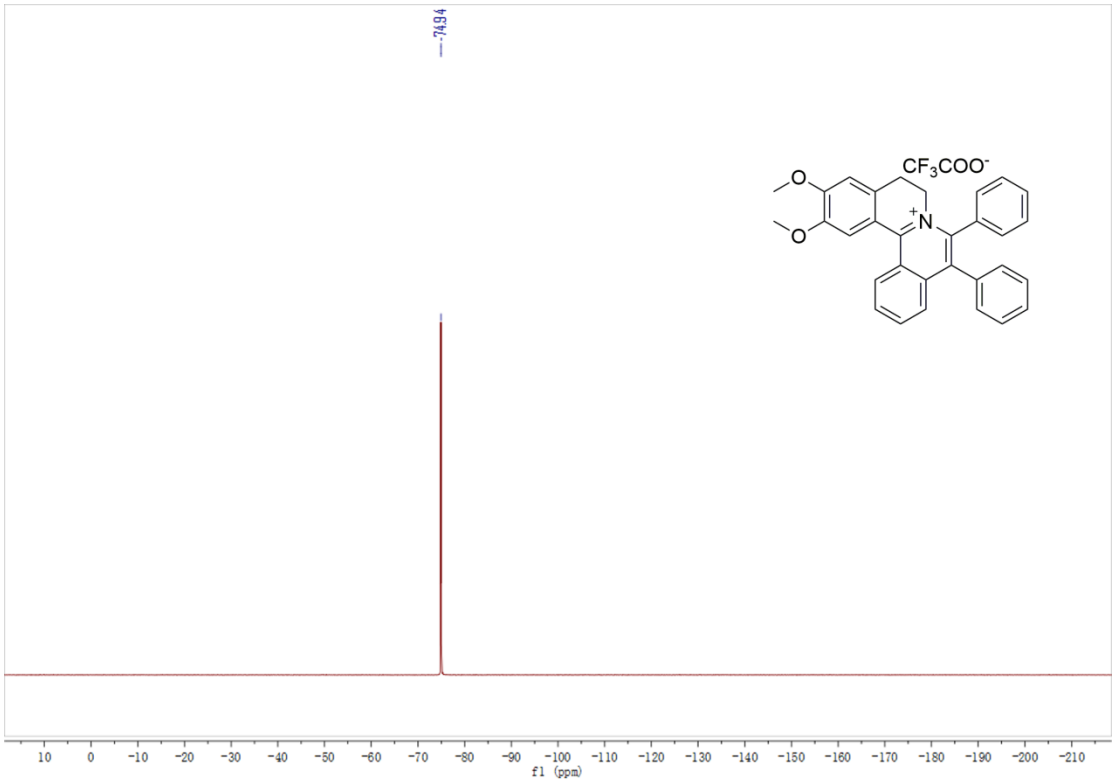

^{19}F NMR spectrum of **LIQ-3** in $CDCl_3$.

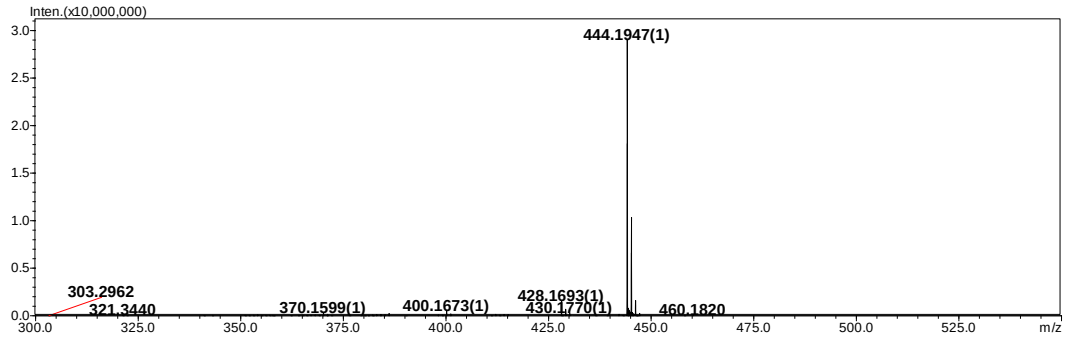

HRMS spectrum of **LIQ-3**.

Reference

1. M. Movassaghi, M. D. Hill, *Org. Lett.*, **2008**, 10, 3485-3488